JAAS

PERSPECTIVE

View Article Online
View Journal | View Issue

Cite this: J. Anal. At. Spectrom., 2016, 31, 1566

Perspective on the use of nanoparticles to improve LIBS analytical performance: nanoparticle enhanced laser induced breakdown spectroscopy (NELIBS)

A. De Giacomo,*[ab] M. Dell'Aglio,[b] R. Gaudiuso,[ab] C. Koral[a] and G. Valenza[ab]

Received 18th May 2016
Accepted 4th July 2016

DOI: 10.1039/c6ja00189k

www.rsc.org/jaas

In this paper, the new approach for Laser Induced Breakdown Spectroscopy (LIBS) based on nanoparticle deposition on the sample surface is reviewed from both fundamental and application points of view. The case of Nanoparticle-Enhanced LIBS (NELIBS) of metal samples is used for describing and discussing the main causes of the emission signal enhancement. A set of test cases is presented, which shows enhancements up to 1–2 orders of magnitude obtained using NELIBS with respect to LIBS. The feasibility and potential of NELIBS are also discussed for several analytical applications, including analysis of metallic samples, transparent samples and aqueous solutions.

1. Introduction

NELIBS (Nanoparticle Enhanced Laser Induced Breakdown Spectroscopy) is a variant of the well-known LIBS technique, and is based on the deposition of metallic nanoparticles (NPs) on the sample surface before laser irradiation, in order to enhance the emission signal during LIBS.

The use of nanostructures as 'spectroscopic enhancers' is getting growing attention for several applications in spectroscopy, microscopy and sensing.[1–3] Many theoretical and experimental studies have demonstrated that when a substrate is irradiated with a laser after NPs have been deposited on its surface, the laser electromagnetic field is locally enhanced and a measurable current due to electron field emission is induced even at relatively low irradiance (around 1 GW cm^{-2}).[4–6] The coupling between the laser electromagnetic field and the surface plasmons of the NPs in contact with a flat surface substrate has been investigated deeply in recent years.[5,6] Nonetheless, so far only a few investigations have focused on the effect of this phenomenon on the production of plasma through the laser–matter interaction in the irradiance regime providing significant ablation. Most studies on this topic have been carried out with ultra-short pulses, which provide a high incident electromagnetic field and at the same time allow protecting the irradiated area of the sample from damage related to the laser breakdown. In contrast, in this paper we review the effect of ns-laser pulses at irradiance between 1 and 10 GW cm^{-2}. In this regime, it is possible to exploit the electromagnetic field enhancement for the laser breakdown of the sample during the ablation process, and to consequently enhance the LIBS signal. Indeed, depositing NPs on the sample surface can strongly affect several aspects of the laser ablation process, which include change of the optical properties of the target surface, introduction of thermally insulated defects into the irradiated area and increase of the laser electromagnetic field due to the laser-induced local plasmonic field of the NPs themselves. Macroscopic changes of the substrate surface properties can affect the plasma formation and, in turn, the optical emission, only to a limited extent (increasing the emission signal up to 2–4 times). On the other hand, the electromagnetic field enhancement can virtually increase the emission signal up to several hundred times with respect to the signal of a sample ablated under normal conditions.[7] Based on this observation, it appears that NELIBS can give a strong boost to LIBS in terms of sensitivity, enabling most of the well-known LIBS advantages[8] also for trace element quantification in laboratory analysis. Of course, the deposition of NPs is in itself a sample preparation procedure, that, though simple and not time consuming, may be difficult or impossible in on-field applications or remote sensing. Nonetheless, the future of NELIBS seems to be promising for laboratory applications where a fast response, minimum sample sacrifice and Limit Of Detection (LOD) at the ppb level are required.

In this paper, examples of critical LIBS experiments with different kinds of samples are discussed and compared with NELIBS, in order to illustrate the great potential of NP use in analytical LIBS, as well as to review the already obtained achievements and suggest further possible developments.

[a]Department of Chemistry, University of Bari, Via Orabona 4, 70125 Bari, Italy. E-mail: alessandro.degiacomo@uniba.it; alessandro.degiacomo@nanotec.cnr.it; Fax: +39 0805929520; Tel: +39 0805442042

[b]Institute of Nanotechnology, CNR-Nanotec, Via Amendola 122/D, 70126 Bari, Italy

2. Experimental set-up

The apparatus for NELIBS experiments is the same as that used in conventional LIBS. The difference is in the experimental procedure, *i.e.* the plasma is generated at the surface of targets where spherical metal NPs have been deposited, by drying one (or more) micro-drop of colloidal solutions with a given concentration. In the experiments described in this work, Ag and Au NPs were used, the drop volume was 1 μl, and the solution concentrations were in the range of 10^{-4} to 10^{-1} mg ml^{-1}.[7] The emission spectra can be acquired with a spectrograph coupled either with a fast ICCD able to work in mono-dimensional (for spectroscopy) and bi-dimensional modes (for imaging) or directly with a time-integrated detection system. To exploit the emission enhancement as much as possible, it is advisable to reduce the plasma image. In this way, the radiation coming from the whole plasma can be collected in the optical fiber aperture or directly in the spectrograph slit. The NP deposition procedure plays a crucial role in the efficiency of NP-induced effects on the ablation process, and thus in the emission enhancement. In the simplest case, that is the one used for all the experiments presented in this work, one drop (1 μl) of colloidal solution is deposited on the sample with a micropipette, and then gently dried by blowing air, so that a dried spot of 2–3 mm in diameter is obtained. More sophisticated methods are also possible to deposit NPs before evaporating the solvent (*e.g.* an electrolyte may be added to the drop of NP colloidal solution to modify the ionic strength of the solution and precipitate NPs, or a suitable capping agent may be used as a spacer to prevent NP agglomeration, *etc.*). In any case, the sample preparation can be very fast and easy, because, as demonstrated in ref. 7, once the optimal surface concentration of NPs is reached, the field enhancement is moderately affected by their concentration in a large range of concentrations (see the next section). Finally, NELIBS works in single shot mode, because after the first shot the NP layer is virtually completely removed by the laser shot itself and by the laser-induced shock wave which also prevents sample contamination by NPs, as discussed in ref. 9 and by the laser-induced shock wave. It is worth underlining that the timescales of NP-mediated ablation (see later on) and of the laser-induced shock wave propagation on a nanometric scale are considerably different (10^{-12} to 10^{-13} s for the first,[10] 10^{-8} to 10^{-7} s for the second). Therefore, in single shot mode they can be considered as completely separated events, but in multi-shot mode the interaction of the subsequent pulses with the substrate would be affected by the partial NP removal due to ablation and shock waves induced by the previous pulses.

These considerations suggest that an easy experimental approach to the sample preparation can be used, which in turn has two practical implications. First of all, an accurate control of NP deposition is not required, once the conditions are properly optimized. Second, the sample is not irreparably contaminated after the NELIBS experiment and is ready for a new measurement by NELIBS or by other analytical techniques.

3. Discussion

As mentioned previously, NELIBS is a variant of the LIBS technique, based on the deposition on the sample surface, before the laser irradiation, of metallic NPs with a suitable interparticle distance. In this view, NELIBS may be included in the category of sample treatments for LIBS.[11] The phenomenon of interest for NELIBS is related to the fact that the laser pulse can induce a coherent oscillation of the conduction electrons in NPs. This in turn amplifies the incident electromagnetic field and the electric field near the particle surface, allowing efficient production of seed electrons through electron field emission. When a metallic sample under laser irradiation has its surface covered with nanoparticles, the electromagnetic field of the incident light[5,6] is hugely increased (1–3 orders of magnitude), and it is possible to obtain direct electron emission from the surface. The competition between multiphoton ionization and electron field emission can be quantified by the Keldysh parameter.[12] The latter allows quick estimation if ionization takes place by absorption of photons, so that electrons can escape through direct or indirect paths of ionization, or if by field emission, by tunneling the work function barrier. The original formalism of the Keldysh parameter is given by the following equation:[12]

$$\gamma = \omega \frac{\sqrt{m_e V_B}}{eF} \quad (1)$$

where V_B is the potential energy of the barrier (*i.e.* the work function potential), F is the electric field intensity, ω is the laser frequency and m_e and e are the electron mass and charge, respectively. If $\gamma > 1$, the main contribution to sample ionization is multiphoton ionization; in contrast, if $\gamma < 1$, the main mechanism is field emission. An example was reported in ref. 7 for LIBS of titanium: considering laser irradiance $= 3 \times 10^8$ W cm^{-2}, electric field intensity $= 10$ MV m^{-1} and work function $=$ 4.33 eV, the Keldysh parameter $\gamma > 10^2$, and as usual multiphoton ionization is the mechanism of free electron production. In contrast, during NELIBS the laser field is enhanced by a factor of 10^2 to 10^3 (ref. 6) as a result of plasmon coupling, thus $\gamma \ll 1$, and the main contribution to free electron production is electron field emission. During the field emission, due to sample heating and electron acceleration upon laser irradiation, the electron flow further increases for the Schottky effect,[13] thus significantly increasing the efficiency of breakdown induction and electron excitation. In this frame, the plasma emission is much more intense with respect to LIBS and the enhancement factor G_{OES} can be used for a systematic comparison between NELIBS and LIBS:

$$G_{OES} = \frac{I_{NELIBS}}{I_{LIBS}} = \frac{N_{0,NELIBS}}{N_{0,LIBS}} \frac{Z(T_{LIBS})}{Z(T_{NELIBS})} \exp\left(\frac{E_u}{k}\left(\frac{1}{T_{LIBS}} - \frac{1}{T_{NELIBS}}\right)\right) \quad (2)$$

The meaning of the terms in eqn (2) is the following: I emission intensity, N_0 total number density of the given emitter,

$Z(T)$ partition function, T plasma temperature, E_u energy of the upper level, and k Boltzmann constant.

Eqn (2) shows clearly that the enhancement is due to two contributions: the first is related to the number of emitters and the second to the different plasma temperature in NELIBS and LIBS.[7] The effect of temperature has been discussed in detail in ref. 7 and 9 and is related to the fact that different enhancement can be found for transitions involving different upper energy levels. Here we will focus our discussion on the enhancement component due to the number of emitters.

In Fig. 1, the total emission image in the case of Ti ablation is reported, and shows that during NELIBS the plasma is much more luminous, which suggests the possibility of much higher sensitivity in the detection of elements. In the following paragraphs, some applications will be discussed in order to show the NELIBS effects in specific analytical cases.

3.1. NELIBS of metals

Metals are for sure the best samples to investigate the basic aspects of NELIBS, because they provide electrical contact with and between the NPs and enable efficient laser–matter coupling. In a first approximation, we can consider that the effect of the change in optical properties of the surface due to the deposition of NPs is negligible with respect to the electromagnetic field enhancement effect. Therefore, the amount of ablated mass becomes directly proportional to the actual laser electromagnetic field[14,15] and consequently the ratio of the ablated mass (and in turn the number of emitters in the plasma) with and without NPs should be directly proportional to the field enhancement. In any case, the enhancement of the electromagnetic field during the laser–matter interaction strongly affects the seed electron production required for plasma induction. As mentioned in the previous section, the Keldysh theory[12] explains how the mechanism of seed electron production changes from the classical photoemission mechanism (*i.e.* multiphoton ionization) to a tunneling one (*i.e.* electron field emission) upon increasing the electromagnetic field on the irradiated sample.[5,7]

The direct production of electrons from the metallic sample (field emission), promoted by the excitation of NP surface plasmons, enhances the breakdown efficiency and thus generates a much more intense plasma. An example of this is shown in Fig. 2a, which compares the emission spectrum of NELIBS and conventional LIBS of Ti, and displays an enhancement of the emission line intensity of about 300 times. It is important to underline that the electrical contact between the NPs and the metallic substrate causes the extraction of electrons by electron field emission to involve a significant portion of the metallic substrate. In turn, this suggests that this method can be a suitable strategy to improve the sensitivity of many laser ablation-based analytical techniques, not only LIBS, but also, for example, LA-ICP and MALDI.[16,17]

In general, the efficiency of the field enhancement depends on two main parameters: laser irradiance, and surface concentration of NPs on the substrate, which is directly related to the packing density.

Fig. 2b shows the effect of laser irradiance on the emission enhancement, G_{OES}, which increases linearly up to a maximum (4 GW cm^{-2} under the experimental conditions employed in this work). At even higher irradiance, the trend inverts and the emission enhancement starts to decrease. This suggests the possible occurrence of non-linear effects responsible for the excitation of electrons within the individual NPs and thus the generation of hot electrons and effective charge separation, which in turn can result in a decrease of the field enhancement.[18]

The trend of the intensity enhancement as a function of NP surface concentration, reported in Fig. 2c, clearly shows a discontinuity between two distinct regimes of breakdown, *i.e.* electron photoemission and electron field emission. Fig. 2c shows that for low NP concentration the main effect on the ablation is due to the NPs acting like thermally insulated defects dispersed on the sample surface. As expected,[19] in this regime the intensity enhancement shows a linear trend with the number of defect points. On the other hand, when a critical surface concentration is reached, an evident discontinuity is observable. At this concentration of NPs, the inter-particle distance becomes effective for inducing the collective oscillation of conduction electrons in NPs upon laser irradiation. Like in Surface-Enhanced Raman Spectroscopy (SERS), there is an optimal value of the packing density, namely the ratio between the diameter of NPs (d) and the inter-particle distance (D). This provides the maximum field enhancement[18,20] and, in turn, the maximum emission signal of the laser induced plasma. This can explain why the enhancement decreases once a certain NP concentration is exceeded. Indeed, when D is short enough to enable the constructive interference of the plasmonic oscillations, the breakdown efficiency depends on the escape of electrons out of the NP surface. At even shorter D, this process can be in competition with electron tunneling through the junction between adjacent NPs.[7] The latter process, in addition to the formation of large agglomerates, can reduce the induced plasmon field enhancement; thus the emission enhancement decreases, as Fig. 2c clearly shows, at high values of the NP surface concentration. Moreover, too many NPs may prevent the laser from actually reaching and effectively ablating the sample surface.

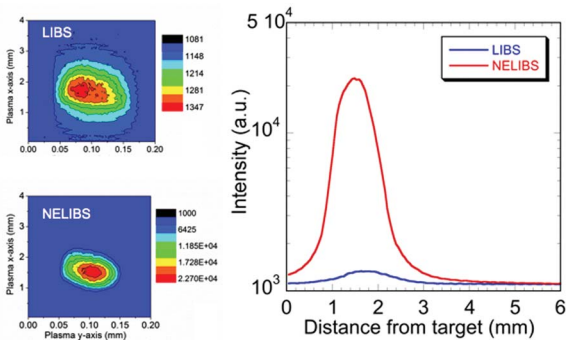

Fig. 1 NELIBS and LIBS emitter spatial distribution: (a) position with respect to the target of spatial distribution maxima as a function of time; (b) typical spatial distribution of emitters (delay time 1800 ns; gate width 50 ns).

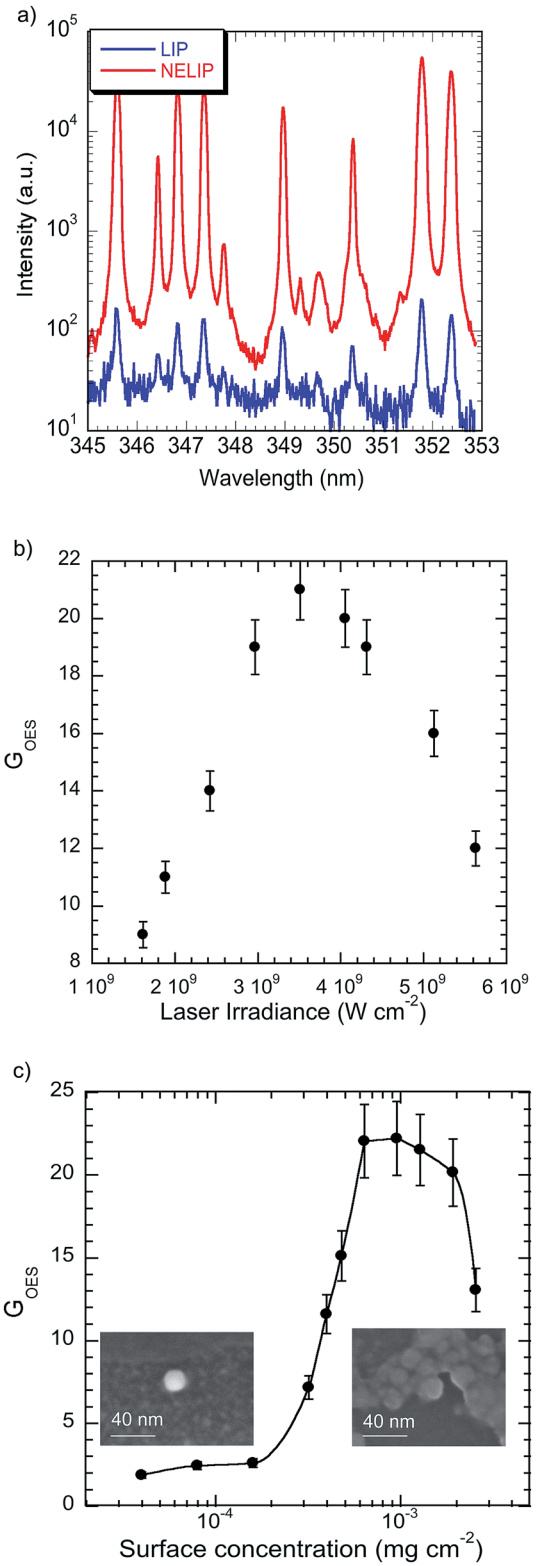

Fig. 2 NELIBS enhancement with respect to LIBS: (a) a frame of the Ti-plasma spectrum (laser irradiance: 8 GW cm^{-2} at 1064 nm; time delay from the laser pulse: 800 ns; gate width: 1 μs). In the case of NELIBS, Ag NPs were deposited on the Ti sample (diameter: 10 nm; surface concentration: 3.5×10^{-4} mg cm^{-2}); (b) emission enhancement, G_{OES}, as a function of laser irradiance. For NELIBS, Ag NPs were deposited on the Ti sample (diameter: 20 nm; surface concentration: 1.6×10^{-3} mg cm^{-2}); (c) emission enhancement, G_{OES}, as a function of the surface concentration of Ag NP (diameter: 10 nm).

The instantaneous generation of seed electrons by field emission enables a multi-point ignition of the plasma and promotes a more homogeneous ablation, as shown by the SEM images reported in ref. 7. On the other hand, this is not the only effect in plasma formation: the significant and instantaneous emission of electrons, caused by the laser and plasmonic field coupling, causes the ions to be further accelerated out of the sample with respect to conventional LIBS. The initial rate of expansion of NELIBS is then increased and the plasma reaches the internal wall of the shockwave produced by the laser–matter interaction[21] at earlier times than with conventional ablation. Therefore, in NELIBS, ions and atoms are back-reflected by the shockwave wall and concentrate at a shorter distance from the target, so that a much higher number density is observed throughout the temporal evolution of the NELIBS plasma with respect to the LIBS one. The higher number density of the NELIBS plasma can cause a faster decrease of the excitation temperature. As a consequence, at the beginning of plasma expansion, the excitation temperature in NELIBS is higher than that in LIBS and within some hundreds of nanoseconds the situation inverts,[22] as reported in Table 1. During the plasma evolution, the enhancement ratio of different transitions is different.[7] For this reason, in order to estimate the actual enhancement, we determined the total number density of emitters in NELIBS and LIBS by assuming a Boltzmann distribution for their population at the experimental temperature.[7,22]

Table 2 shows the dependence of the intensity enhancement on laser wavelength. It is interesting to note that at the wavelengths used in this work, the dependence of the NELIBS signal on wavelength is moderate, while in LIBS it is more marked. This observation is related to the mechanism of breakdown initiation. Electron photoemission (that is the ignition process in LIBS) is strongly affected by the dependence of the absorption coefficient on the incident wavelength. In contrast, in NELIBS the main phenomenon is the collective electron oscillation induced in the NPs by the laser beam, and this mainly depends on the amplitude of the laser electromagnetic field, with no need for the laser wavelength to be in optical resonance with the surface plasmon one.

From the analytical point of view, this discussion implies that it is possible to strongly enhance the LIBS performance in the element detection in metal alloys.[9] As an example, in Fig. 3 the comparison of the calibration curves of Mn and Pb in the case of a copper-based alloy (taken from ref. 9) is reported. It is evident that, during NELIBS, the sensitivity and LOD are enhanced by more than one order of magnitude, allowing the detection of trace elements with a better accuracy than with conventional LIBS. Interested readers may find further examples in ref. 7 and 9.

3.2. NELIBS of transparent media

Transparent media, such as glass, have always been considered challenging for LIBS because the focused laser pulse can penetrate through the sample and cause cracks and poor reproducibility.[23] In this specific case, depositing nanoparticles on the surface can provide several advantages, because the laser

Table 1 Boltzmann plot analysis of NELIBS and LIBS at different time delays from the laser pulse and gate width of 500 ns, at a laser irradiance of 1.5 GW cm^{-2} at 1064 nm (for NELIP 3.5×10^{-4} mg cm^{-2} of 20 nm diameter Ag NPs) from ref. 22

Delay (ns)	NELIP T_{ex} (K)	LIP T_{ex} (K)	NELIP $K \times N_{TOT}$ (cm^{-3})	LIP $K \times N_{TOT}$ (cm^{-3})
800	14 300 ± 1200	10 500 ± 900	7.9×10^{18}	6.5×10^{16}
1300	8700 ± 900	10 400 ± 900	8.0×10^{18}	3.8×10^{16}
1800	8400 ± 800	10 400 ± 900	5.5×10^{18}	2.4×10^{16}

Table 2 Effect of laser wavelength on excitation temperature and total number density of emitters in NELIBS and LIBS (laser irradiance is 1 GW cm^{-2}; delay time 800 ns, gate width 5 μs; for NELIP, 3.5×10^{-4} mg cm^{-2} of 20 nm diameter Ag NPs). The temperature was obtained by the slope of the Boltzmann line and the relative total number density was estimated by the intercept and the partition function at the experimental temperature, while K is an instrumental constant. The fraction of ionized emitters was calculated by the Saha equation at the experimental temperature

Laser wavelength (nm)	NELIP T_{ex} (K)	LIP T_{ex} (K)	NELIP $K \times N_{TOT}$ (cm^{-3})	LIP $K \times N_{TOT}$ (cm^{-3})
355	7600 ± 900	6300 ± 600	4.7×10^{18}	1.4×10^{17}
532	9100 ± 900	8600 ± 900	4.5×10^{18}	3.0×10^{17}
1064	11 000 ± 1000	8200 ± 800	6.6×10^{18}	1.5×10^{18}

pulse couples with the deposited NPs rather than directly interacting with the glass, as shown in Fig. 4. In this case, where the substrate is not conductive, the electron field emission due to the laser field enhancement can only involve the layers of the substrate that are in direct contact with the deposited NPs. Therefore, thanks to the NP mediation, the laser–glass coupling is made possible only at the very sample surface, and at much lower irradiance than in normal LIBS.[11] The result is that an intense plasma is generated on the glass surface, providing information about the elemental composition of the most superficial layers of the glass sample.

As mentioned previously, the presence of NPs allows inducing the plasma at the glass surface at much lower irradiance than in common LIBS. Thus, a larger laser spot can be used, allowing a much gentler ablation and preventing cracks. Moreover, using a larger spot (in our experiments, about 2 mm) has one further advantage, *i.e.* benefiting from the enhancing effect of a higher number of NPs.

Fig. 5 shows a comparison between NELIBS and LIBS spectra of borosilicate glass, obtained with a 532 nm laser pulse and an irradiance of 0.8 GW cm^{-2}. While the LIBS spectrum under these experimental conditions does not contain any signal, the NELIBS spectrum clearly shows measurable peaks. It is interesting that, as observed for metals, once a certain critical concentration of NPs is reached, the glass emission signal does not appear to have a strong dependence on the NP concentration. Moreover with conventional LIBS, in order to achieve the same spectral intensity of the NELIBS spectrum, a much higher irradiance is required (about 3 times), with the other

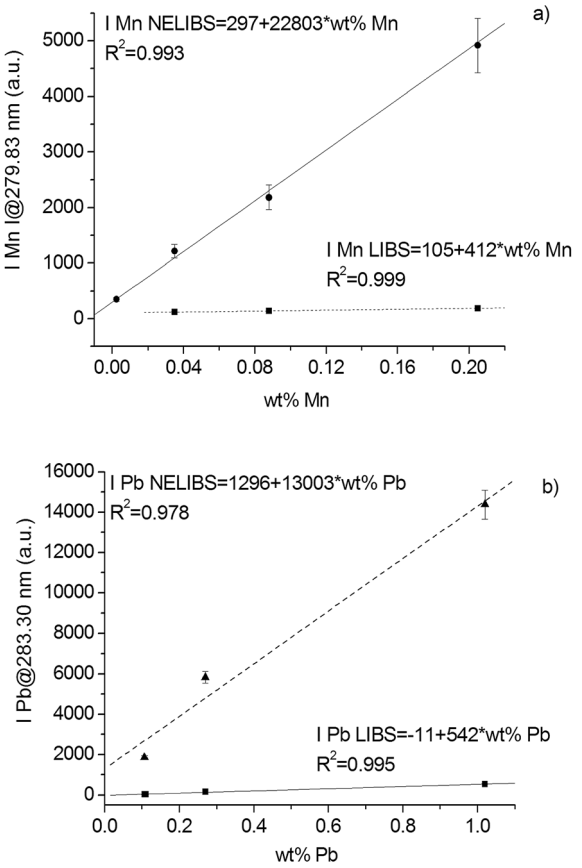

Fig. 3 An example from ref. 9 of comparison between the LIBS and NELIBS calibration lines of (a) Mn and (b) Pb contained in copper-based alloys.

experimental parameters kept unchanged. As a consequence, the sample damage induced by LIBS is much higher, while the gentler ablation regime enabled by NELIBS can better preserve the sample. For its peculiar non-destructivity, this technique may be successfully applied to the analysis of precious transparent samples, such as artistic or archaeological glasses and gemstones.

3.3. NELIBS of liquid solutions

The NP effect on LIBS of non-conducting samples can also be exploited in a different way, *i.e.* for enhancing the signal of analytes deposited on top of the NP layer, rather than that of substrates below them, as in the examples discussed so far. This is for example the case of the analysis of micro-drops of liquid solutions.[24,25] As is well known, solutions can be successfully analyzed by LIBS either directly in the liquid phase by Double Pulse (DP) techniques or by depositing and drying drops of solution on a substrate. While DP-LIBS enables analysis of solutions down to ppm levels,[26] the method of drying several drops of solution virtually does not have any LOD limitation, as far as there is no restriction in the available amount of solution. In contrast, if only a few microliters of solution are available for the analysis, sensitivity can become a major issue in LIBS analyses. In these cases, the use of NPs can strongly improve the

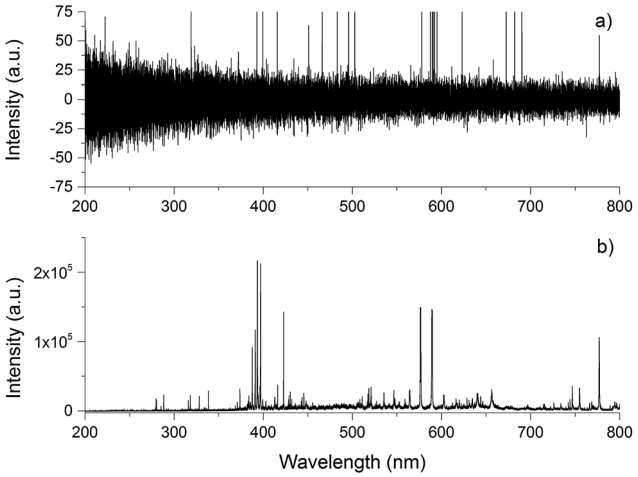

Fig. 4 LIBS and NELIBS of glasses. The spectra were obtained with $F = 8$ J cm^{-2}. For NELIBS, AgNPs were deposited on the glass surface (diameter: 20 nm; surface concentration: 0.15 mg cm^{-2}).

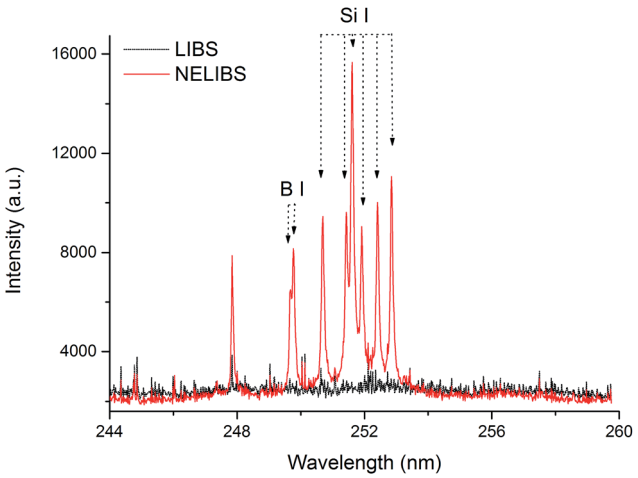

Fig. 5 Comparison between LIBS and NELIBS of borosilicate glass. $I = 1.3$ GW cm^{-2}. For NELIBS, Ag NPs were deposited on the glass surface (diameter: 20 nm; surface concentration: 0.15 mg cm^{-2}).

LIBS sensitivity enabling sub-ppb level measurements. In this further variant of NELIBS, one drop of NP solution is deposited and dried on a non-conducting substrate prior to dropping the analyte solution. In this way, the field enhancement effect can involve the analyte species deposited on the NP layer. Fig. 6 shows the calibration curve of Ag (Ag I, 328.068 nm), in 1 μl of $AgNO_3$ solution. It can be noted that concentrations as low as few hundreds of ppt can be measured by NELIBS, while in the case of LIBS the LOD was in the order of hundreds of ppb.[25]

In this case, in addition to the electromagnetic field enhancement described in the previous sections, two further advantages arise. First of all, the adsorption of solution analytes on the NP surface, which ensures that virtually all the deposited analytes are transferred to the plasma phase with one single laser shot. Moreover, with conventional LIBS the mass of the dried solution is very low (about 1 ng) and the LIBS plasma becomes weak because it contains few material particles (atoms, ions and electrons). In contrast, in NELIBS the NPs feed the plasma with atoms, ions and electrons generated by the ablation of NPs themselves; thus a more intense and stable plasma is produced.

Another case of particular interest is the detection of metals in biological media which by using LIBS is rather challenging, because when ablating organic or biological molecules, the high amount of atoms difficult to ionize (carbon, nitrogen *etc.*) can lead to important plasma quenching. As an example, the comparison between NELIBS and LIBS spectra of a solution of the Reaction Center from the purple bacterium *Rhodobacter sphaeroides* is shown in Fig. 7. This protein was treated with alkali metal salts. After extensive dialysis, the native functionality was restored and all the cations were removed, except Li. LIBS and NELIBS were then used for detecting the Li content.[25,27] An enhancement of one order of magnitude was observed for Li emission lines at 671 nm when NPs were

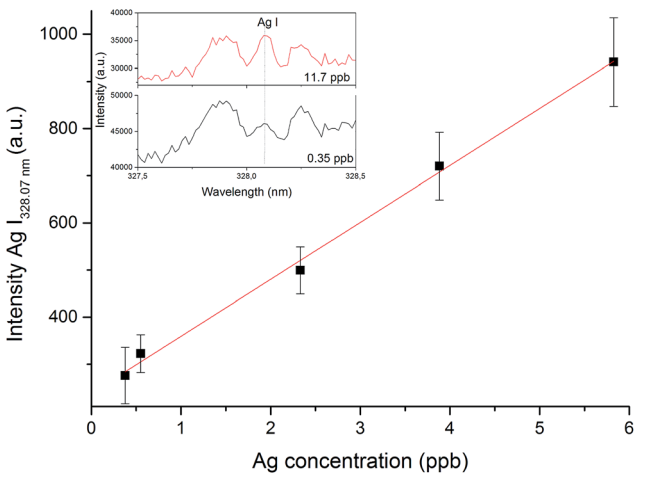

Fig. 6 NELIBS microdrop calibration curve of Ag I at 328.07 nm from ref. 25. Laser irradiance of 8 GW cm^{-2}, Au NPs (1 μl, 0.03 mg ml^{-1}).

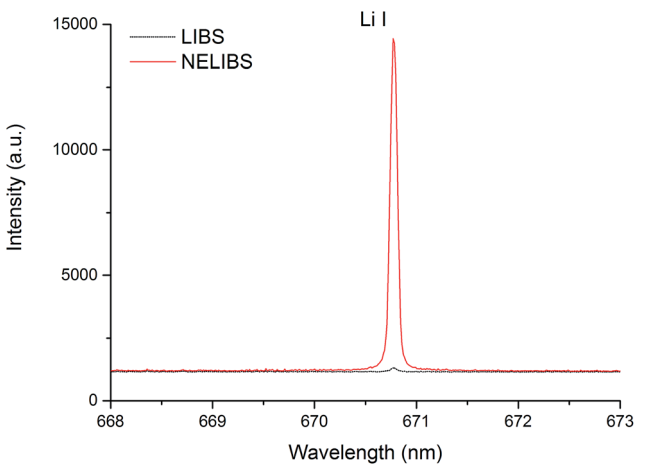

Fig. 7 Comparison between NELIBS and LIBS Li signals in a solution of the protein Reaction Center (RC) from the purple bacterium *Rhodobacter sphaeroides* at a concentration of 10^{-5} M.[25]

deposited, thus enabling the Li content quantification using the calibration curve method. The same approach was extended to the quantitative analysis of metals in human serum.[25] These latter examples appear to open the way for promising applications in medical and forensic applications of LIBS.

4. Conclusion

In this paper, the use of NP deposition on the sample surface for LIBS analysis was discussed, both from the fundamental and application points of view. Three different typologies of NELIBS experiments were presented, *i.e.* metals, glasses and liquid solutions, demonstrating the efficiency of NELIBS with respect to conventional LIBS. The main causes of the enhancement are related to the better ablation efficiency when the laser electromagnetic field couples with the induced NP plasmonic field. At the same time, an important role is played by the injection of atoms and ions provided by the breakdown of NPs themselves, when a small amount of sample is analyzed by LIBS. The overall results suggest the impressive potential of NP use in LIBS, as well as in other laser ablation-based techniques, at least for what concerns laboratory applications.

Acknowledgements

The authors are grateful to Mr Erik Kepes and Mr Martin Mazura from Brno University of Technology and to Prof. Gerardo Palazzo, Prof. Fabio Arnesano and Dr Vincenzo Mangini from the University of Bari. This research is partially supported by MIUR under the project PON SISTEMA.

References

1 S. Nie and S. R. Emory, Probing Single Molecules and Single Nanoparticles by Surface-Enhanced Raman Scattering, *Science*, 1997, **275**(5303), 1102–1106.
2 F. C. Adams and C. Barbante, Nanoscience, Nanotechnology and Spectrometry, *Spectrochim. Acta, Part B*, 2013, **86**, 3–13.
3 S. Kühn, U. Håkanson, L. Rogobete and V. Sandoghdar, Enhancement of single-molecule fluorescence using a gold nanoparticle as an optical nanoantenna, *Phys. Rev. Lett.*, 2006, **97**, 017402.
4 S. M. Teichmann, P. Rácz, M. F. Ciappina, J. A. Pérez-Hernández, A. Thai, J. Fekete, A. Y. Elezzabi, L. Veisz, J. Biegert and P. Dombi, Strong-field plasmonic photoemission in the mid-IR at <1 GW/cm^2 intensity, *Sci. Rep.*, 2015, **5**, 7584.
5 T. Turker and F. Robicheaux, Dichotomy between tunneling and multiphoton ionization in atomic photoionization: Keldysh parameter γ *versus* scaled frequency Ω, *Phys. Rev. A*, 2012, **86**, 053407.
6 F. Schertz, M. Schmelzeisen, M. Kreiter, H. J. Elmers and G. Schonhense, Field Emission Effect Generated by the Near Field of Strongly Coupled Plasmons, *Phys. Rev. Lett.*, 2012, **108**(237602), 1–5.
7 A. De Giacomo, R. Gaudiuso, C. Koral, M. Dell'Aglio and O. De Pascale, Nanoparticle Enhanced Laser Induced Breakdown Spectroscopy: Effect of nanoparticles deposited on sample surface on laser ablation and plasma emission, *Spectrochim. Acta, Part B*, 2014, **98**, 19–27.
8 F. J. Fortes, J. Moros, P. Lucena, L. M. Cabalín and J. J. Laserna, Laser-induced breakdown spectroscopy, *Anal. Chem.*, 2013, **85**(2), 640–669.
9 A. De Giacomo, R. Gaudiuso, C. Koral, M. Dell'Aglio and O. De Pascale, Nanoparticles Enhanced Laser Induced Breakdown Spectroscopy on metallic samples, *Anal. Chem.*, 2013, **85**, 10180–10187.
10 S. Liang, *Quantum tunneling and field electron emission theories*, World Scientific Publishing Co. Pte. Ltd., Singapore, 2014.
11 S. C. Jantzi, V. Motto-Ros, F. Trichard, Y. Markushin, N. Melikechi and A. De Giacomo, Sample treatment and preparation for laser-induced breakdown spectroscopy, *Spectrochim. Acta, Part B*, 2016, **115**, 52–63.
12 L. V. Keldysh, Ionization in the field of a strong electromagnetic wave, *Sov. Phys. - JETP*, 1965, **20**/**5**, 1307–1314.
13 A. J. Dekker, *Solid State Physics*, Prentice-Hall, Inc., Englewood Cliffs, New Jersey, 1957, pp. 220–226.
14 R. Fabbro, E. Fabre, F. Amiranoff, C. Garban-Labaune, J. Virmont, M. Weinfeld and C. E. Max, Laser-wavelength dependence of mass ablation rate and heat-flux inhibition in laser produced plasmas, *Phys. Rev. A*, 1980, **26**, 2289.
15 K. Dittrich and R. Wennrich, Laser vaporization in atomic spectroscopy, *Prog. Anal. At. Spectrosc.*, 1984, **7**, 193–198.
16 V. Amendola, L. Litti and M. Meneghetti, LDI-MS Assisted by Chemical-Free Gold Nanoparticles: Enhanced Sensitivity and Reduced Background in the Low-Mass Region, *Anal. Chem.*, 2013, **85**, 11747–11754.
17 J. A. McLean, K. A. Stumpo and D. H. Russell, Size-selected (2-10 nm) gold nanoparticles for matrix assisted laser desorption ionization of peptides, *J. Am. Chem. Soc.*, 2005, **127**(15), 5304–5305.
18 D. C. Marinica, A. K. Kazansky, P. Nordlander, J. Aizpurua and A. G. Borisov, Quantum Plasmonics: Nonlinear Effects in the Field Enhancement of Plasmonic Nanoparticle Dimer, *Nano Lett.*, 2012, **12**, 1333–1339.
19 C. T. Walters, R. H. Barnes and R. E. Beverly, Initiation of Laser supported detonation (LSD) waves, *J. Appl. Phys.*, 1978, **49**/**5**, 2937–2949.
20 M. K. Kinnan and G. Chumanov, Plasmon Coupling in Two-Dimensional Arrays of Silver Nanoparticles: II. Effect of the Particle Size and Interparticle Distance, *J. Phys. Chem. C*, 2010, **114**, 7496–7501.
21 A. De Giacomo, M. Dell'Aglio, R. Gaudiuso, S. Amoruso and O. De Pascale, Effects of the background environment on formation, evolution and emission spectra of laser-induced plasmas, *Spectrochim. Acta, Part B*, 2012, **78**, 1–19.
22 C. Koral, A. De Giacomo, X. Mao, V. Zorba and R. E. Russo, Nanoparticle Enhanced Laser Induced Breakdown for Improving the Detection of Molecular Bands, *Spectrochim. Acta, Part B*, submitted.
23 C. Barnett, E. Cahoon and J. R. Almirall, Wavelength dependence on the elemental analysis of glass by Laser

Induced Breakdown Spectroscopy, *Spectrochim. Acta, Part B*, 2008, **63**(10), 1016–1023.

24 D. A. Rusak, T. P. Anthony and Z. T. Bell, Note: A novel technique for analysis of aqueous solutions by laser-induced breakdown spectroscopy, *Rev. Sci. Instrum.*, 2015, **86**((11)), 116106.

25 A. De Giacomo, C. Koral, G. Valenza, R. Gaudiuso and M. Dell'Aglio, Nanoparticle Enhanced Laser-Induced Breakdown Spectroscopy for Microdrop Analysis at subppm Level, *Anal. Chem.*, 2016, **88**(10), 5251–5257.

26 A. De Giacomo, M. Dell'Aglio, O. De Pascale and M. Capitelli, From single pulse to double pulse ns-Laser Induced Breakdown Spectroscopy under water: Elemental analysis of aqueous solutions and submerged solid samples, *Spectrochim. Acta, Part B*, 2007, **62**, 721–738.

27 M. Giustini, M. Parente, A. Mallardi and G. Palazzo, Effect of Ionic Strength on Intra-protein Electron Transfer Reactions: the Case Study of Charge Recombination within the Bacterial Reaction Center, *Biochim. Biophys. Acta, Bioenerg.*, 2016, **1857**(9), 1541–1549.